Renewable and Sustainable Energy Reviews 14 (2010) 2249–2255

Contents lists available at ScienceDirect

Renewable and Sustainable Energy Reviews

journal homepage: www.elsevier.com/locate/rser

Performance of solar chimney power plant in Qinghai-Tibet Plateau

Xinping Zhou [a,b,*], Fang Wang [a,b], Jian Fan [b], Reccab M. Ochieng [c]

[a] Department of Mechanics, School of Civil Engineering and Mechanics, Huazhong University of Science and Technology, Luoyu Road 1037, Wuhan, Hubei 430074, PR China
[b] Hubei Key Laboratory for Engineering Structural Analysis and Safety Assessment, Huazhong University of Science and Technology, Luoyu Road 1037, Wuhan, Hubei 430074, PR China
[c] Department of Physics and Materials Science, Maseno University, P.O. Box 333, Maseno, Kenya

ARTICLE INFO

Article history:
Received 1 April 2010
Accepted 20 April 2010

Keywords:
Solar chimney
Power generation
Solar collector
Qinghai-Tibet Plateau

ABSTRACT

A solar chimney power plant (SCPP) is proposed to be built in Qinghai-Tibet Plateau where there is abundant solar radiation, high direct solar radiation low atmospheric temperature, large diurnal temperature range, and lots of salt lakes working as heat storage system, which can help to improve the power output of SCPP. The plant is expected to power local railway traffic lines and act as a solar power base to supply power for national development. The performance of the SCPP that will be built in Qinghai-Tibet Plateau is analyzed and power potential estimated by developing a simple mathematical model. It is found that SCPP if built in the plateau can produce twice more power than an SCPP built on the same latitude of other regions. The yearly power potential for SCPP in Qinghai-Tibet Plateau is estimated to be 86.8 million TJ. When 10–20% of the plateau land is used for the SCPP, the yearly power output may reach 8.7 million TJ to 17.4 million TJ, accounting for 10.7–21.3% of China's energy consumption in 2008 which stood at 81.6 million TJ. It is found that the SCPP in the plateau can support local and national development together with other renewable energy resources such as hydroelectric power and wind power.

Contents

1. Introduction

Large-scale western development policy has entered the implementation phase in China in the recent years. However, the western regions of China are usually high-elevation areas and far away from the developed eastern regions. It is important part of the project of large-scale western development to build expedient traffic lines to link the western regions and the developed eastern regions. The famous Qinghai-Tibet Railway from the Xining, Qihai, to Lhasa, Tibet, located in Qinghai-Tibet Plateau, was built and started to be used on July 1, 2006, which had a span of 1956 km and mean elevation of more than 4000 m [1]. Since the electric network is hard to power, the trains in the high and remote Qinghai-Tibet Plateau are driven by diesel transported from Sinkiang. In the high-elevation railway regions, air is very thin. This causes incomplete combustion of the diesel and the diesel engines work at nearly half their efficiencies. Two or more diesel locomotives are always needed to pull the trains and this requires much more energy than using electric network. Furthermore, rapid development of the global economy and increase in population and living standards

* Corresponding author at: Department of Mechanics, School of Civil Engineering and Mechanics, Huazhong University of Science and Technology, Luoyu Road 1037, Wuhan, Hubei 430074, PR China. Tel.: +86 27 62250811; fax: +86 27 87542221.
E-mail addresses: xpzhou08@mail.hust.edu.cn, zhxpmark@hotmail.com (X. Zhou).

1364-0321/$ – see front matter © 2010 Elsevier Ltd. All rights reserved.
doi:10.1016/j.rser.2010.04.017

have been posing great pressure on energy resources and the environment in China [2]. Accordingly, to utilize the local renewable energy sources to generate electric power to run the railway traffic lines and supply the rest to the developed regions by high-voltage lines is an effective measure to promote local and national development. In China, annual global solar radiation increases gradually from the Northeast to Southwest regions. Maximum annual solar radiation in excess of 6500 MJ/m^2 is found in Qinghai-Tibet Plateau (Fig. 1) where less sunlight is scattered by thin air and the path travelled by the rays is short. It is difficult for the thin air to block the ground reflection such that local atmospheric temperature is low [3–5]. SCPP is therefore a good choice for utilizing local solar radiation, where a solar collector is used to store solar radiation and a chimney drives the airflow to the turbine generators to generate electricity assisted by temperature difference of the collector air and the ambient [6]. China's Railways Ministry has shown great interest in this solar chimney power technology.

By using a simple mathematical model developed based on energy balance, the performance of SCPP in Qinghai-Tibet Plateau is analyzed, and compared with other regions, and the power potential of SCPP in this plateau is estimated in this paper.

2. Description of SCPP

The concept of SCPP was first described in a publication written by a German author, Günther in 1931 [7]. SCPP utilizes solar energy to produce ventilation that drives air turbines to produce electric power. The technology combines three components: a collector, a chimney and air turbines [8]. In the collector, solar radiation is used to heat an absorber (ordinarily soil or water bags [9]) on the ground, and then a large body of air, heated by the absorber, rises up the chimney, due to the density difference from the air inside the chimney and the ambient air. The rising air drives turbines installed at the chimney base to generate electricity (see Fig. 2). The solar collector produces greenhouse effect to store solar energy. High chimney produces driving force of airflow together with the temperature difference of the collector air and the ambient. Proposed by Schlaich in 1978, a pilot experimental setup, the Manzanares prototype plant was built [1,10–11]; the Connecticut setup [12], the Izmit setup [13], the Florida setup [14], the Wuhan setup [15], the Botswana setup [16], the Brazil setup [17], and the Isparta setup [18] were built up and tested, and some investigations were done on them. Their parameters are presented in Table 1. The characteristics of the SCPP are: (1) Operation cost is low. (2) Cooling water is not needed. (3) Construction technology is familiar, and materials are abundant and cheap. (4) Soil layer under the collector roof can work as natural energy storage system. (5) Both direct and diffuse solar radiations are utilized. The major concentrating solar thermal power plants (e.g. solar trough plant, solar tower plant, and solar dish plant), often driven by high-temperature steam produced from solar concentrators, can only use direct radiation. Thus SCPP can operate on clear and overcast days and nighttime affected by its fourth and fifth features. (6) The SCPP energy conversion efficiency is lower than other renewable energy power systems, but can be improved by increasing its dimension. SCPP is designed to produce electric power on a large scale. For commercial power plant producing energy economically, not only is a large collector area necessary for collecting solar energy, but also a high gigantic chimney is required to house a big turbine and to obtain a large driving force.

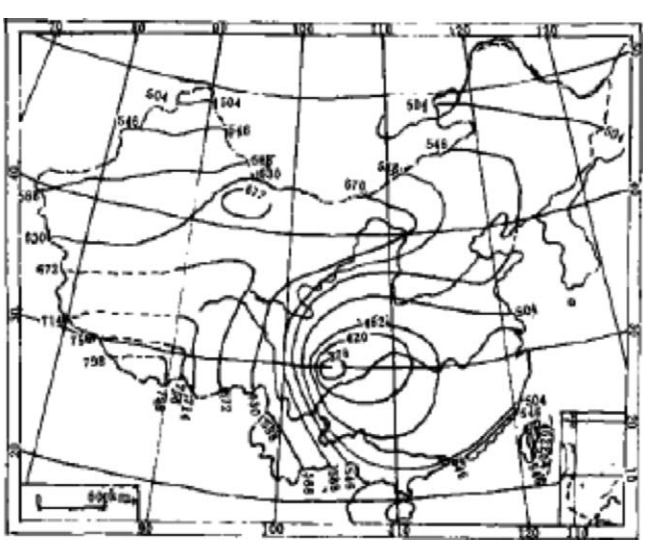

Fig. 1. Graph of annual solar global radiation in regions of China [3,5] (unit: kJ/cm^2).

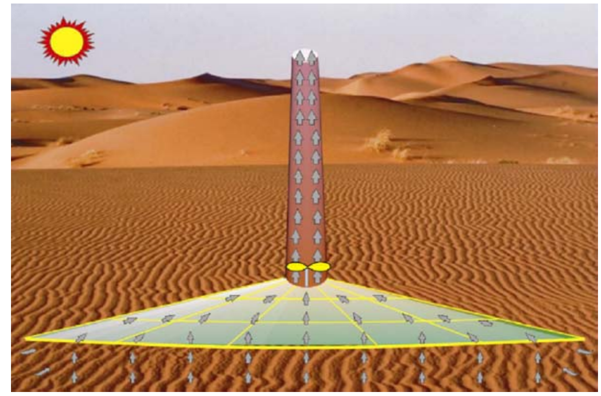

Fig. 2. Schematic diagram of SCPP.

A salt gradient solar pond is usually a solar energy storage system which collects solar radiation and stores it in the brine in form of thermal energy for a long period of time, whose temperature could reach >100 °C. Salt lake is a natural solar pond, which can be used as heat storage system for SCPP to give a much more uniform daily output profile [19–21].

3. SCPP in Qinghai-Tibet Plateau

Most parts of Qinghai-Tibet Plateau (longitude between E74° and E104°, Latitude between N25° and N40°), the largest plateau in China and the highest plateau in the world, are located in Southwest China, including Tibet, Qinghai, Western Sichuan, Southern Sinkiang, and some regions in Gansu and Yunnan, which covers 2.57 million km^2, accounting for 26.8% of the total land of China (Fig. 3) [22]. This plateau is called the Tibet Roof of the World, with mean elevation ranging from 4000 to 5000 m, which is surrounded by many high mountains more than 6000 m in elevation, such as the Kunlun Shan, Tian Shan, Qilian Shan, Hengduan Shan. This plateau is also divided into many basins and

Table 1
Parameters of pilot experimental SCPP setups [1,10–18].

Setup	Chimney height/m	Collector diameter or area	Power/kW
Manzanares prototype	194.6	244 m	50
Connecticut setup	10	6 m	–
Izmit setup	2	9 m^2	–
Florida setup	7.92	9.15 m and 18.3 m	–
Wuhan setup	8.8	10 m	–
Botswana setup	22	160 m^2	–
Brazil setup	11	25 m	–
Isparta setup	15	16 m	–

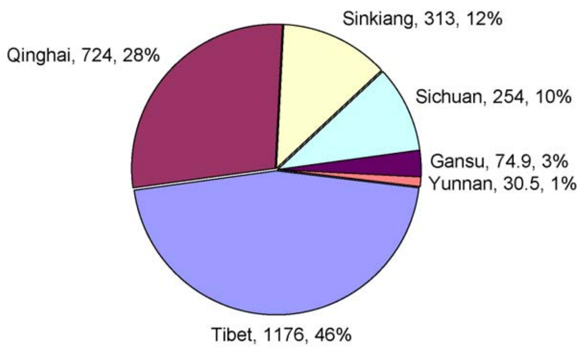

Fig. 3. Districts covered of Qinghai-Tibet Plateau and their area (thousand km^2) [22].

open valleys created by inner mountains such as Danggula Shan, Gangdise Shan and Nyainqentanglha Shan.

Annual global solar radiation of the major regions of Qinghai-Tibet Plateau is more than 6500 MJ/m^2, and sunshine duration lies between 2500 h and 3600 h per year. The annual global solar radiation and atmospheric temperature of the plateau were compared with other regions by taking nine regions of Qinghai-Tibet Plateau and ten regions out of the Plateau as examples (Table 2). The results shows that the annual global solar radiation of the regions in the Qinghai-Tibet Plateau is much more than the other regions with almost the same latitude, for example, the annual global solar radiation in Lhasa, Gerze, or Qaidam and others is twice as much as at Xi'an, Chengdu, Guiyang, which have the almost same latitude. However, the average annual atmospheric temperature is lower.

Direct solar radiation is the main part of global solar radiation in the plateau, with the percentage lying between 55% and 78%. The largest values are found in Southern and Western Tibet (e.g. Shiquanhe with 78%, Lhasa with 69%), larger values in Qaidam basin (e.g. Gomud with 61%), and the lowest values in Nagqu-Yushu Plateau and Southeast Tibet, lie between 55% and 57%. The values are usually higher than the same latitude regions, such as Shanghai with a value of 50%, Xi'an with 47%, Yichang with 45%, Chongqing with 39% and Chengdu with 32%.

A survey of the diurnal temperature ranges of plateau climate, mountain climate, mainland climate, and marine climate found that the diurnal temperature ranges of plateau is the highest due to high elevation and thin air. For diurnal temperature range, Qinghai-Tibet Plateau can be separated into two parts: high-value regions in Qaidam basin, Ali area, Nagqu, Tingri, Hainan Tibetan Autonomous Prefecture, Golog Tibetan Autonomous Prefecture where annual diurnal temperature ranges are often higher than 17 °C (e.g. annual diurnal temperature range can reach up to 17.7 °C in Lenghu, Qinghai province), and the low-value regions where annual diurnal temperature ranges are lower than 14 °C, but higher than the same latitude regions not in Qinghai-Tibet Plateau [4].

There are many salt lakes located in the Qinghai-Tibet Plateau that can be used to ensure the efficient operation of SCPP by using them as heat storage systems during cloudy days and at night. As can be seen in Table 3, salt lake area in Tibet and Qinghai accounts for 68.35% of the total area in China. Qinghai Lake, the largest salt lake is located in Qinghai, having an area of 4456 km^2. Nam Lake, the highest salt lake is located in Tibet, having an area of about 2000 km^2 at an elevation of 4650 m [23]. In the table, only the inland salt lakes with areas of more than 1 km^2 were recorded.

The unique features of building SCPP in Qinghai-Tibet Plateau are:

1. Nearly no person and industry will be affected by the SCPP in Qinghai-Tibet Plateau which is sparsely populated.
2. The land is vast, relatively flat and barren, which is suitable for SCPP location, despite high-elevation. Free use of uncultivated deserts and barren mountains will avoid purchasing land for the establishment and construction sites for solar collector and provide an effective approach to the exploitation of uncultivated and barren regions. Furthermore, abundant solar radiation is an important factor to improve the power output of SCPP in the plateau. Both high direct solar radiation and low ambient

Table 3
Distribution of salt lakes in China's regions [23].

Region	Number of salt lakes	Percent to total number/%	Area/km^2	Percent to total area/%
Tibet	234	28.78	8150.18	20.53
Qinghai	71	8.73	18,986.38	47.82
Sinkiang	112	13.78	10,789.56	27.18
Inner	375	46.12	1441.2	3.63
Jilin	2	0.25	63.8	0.16
Hebei	2	0.25	54.7	0.14
Shanxi 1*	1	0.12	92	0.23
Shanxi 2*	9	1.11	52.1	0.13
Ningxia	4	0.49	19.38	0.05
Gansu	3	0.37	53	0.13
Total	813	100	39,702.3	100

* In China, there are two Shanxi Province, i. e., Shanxi 1 and Shanxi 2.

Table 2
Annual global solar radiation and atmospheric temperature of some cities in and out of Qinghai-Tibet Plateau [3,4].

Region	Longitude	Latitude	Mean elevation/m	Annual solar radiation/MJ/m^2	Average annual atmospheric temperature/°C
Lhasa	E91°06′	N29°36′	3650	7802.8	8.9
Gerze	E81°59′–86°	N31°30′–35°40′	4700	7565.8	−0.2
Qamdo	E96°51′	N31°15′	3500	6552	7.6
Bange Lake	E89°29′	N31°43′	4522	8274	−1.4
Qaidam	E90°16′–99°16′	N35–39°20′	2600–3000	7770	5.5
Gomud	E94°53′24	N36°25′12	2807	6930	−4.2
Xining	E101°49′17″	N36°34′3″	2261	6105	5.7
Yushu	E89°27′–97°39′	N31°45′–36°10′	4200	6720	−0.8
Lenghu	E92°88′–94°30′	N37°46′–39°18′	2783	7447	2.6
Urumqi	E86°37′33″–88°58′24″	N42°45′32″–44°08′	800	5964	7.5
Hohhot	E110°46′–112°10′	N40°51′–41°8′	1040	6090	7.7
Shenyang	E123°24′	N41°48′	<500	4956	8
Beijing	E116°23′29″	N39°54′20″	<500	5586	13.2
Jinan	E117°	N36°40′	<500	5292	14.4
Nanjing	E118°22″–119°14″	N31°14″–32°37″	<500	4914	16.3
Shanghai	E121°29′	N31°14′	<500	4851	17.1
Xi'an	E108°54′39″	N34°13′58″	<500	3948	15
Chengdu	E102°54′–104°53′	N30°05′–31°26′	500	3738	16.2
Guiyang	E106° 07′–107°17′	N26°11′–27°22′	1071	3819	14.1

temperatures can help to improve the conversion efficiency of SCPPs. Large diurnal temperature ranges, helping in the continuous operation of the turbines after sunset are also another valuable resource for solar chimney power generation. Lots of salt lakes in the plateau can be used as heat storage system for SCPP to give a much more uniform daily power output profile and increase the total power output by enlarging receiving surface of solar radiation.
3. SCPP can help in local ecological restoration [24–25], thus lessening soil erosion and disasters from floods in the lower reaches of some rivers, e.g., Yangtze River, which have their sources in the Qinghai-Tibet Plateau.
4. SCPP can power the local railway traffic lines and supply the rest of the power to the developed eastern regions by acting as the solar power base of China.
5. Solar chimney power generating industry can promote the local and national social progress, and guarantee social–economic stability.

4. Mathematical model

Energy conversion by SCPP can be divided into three phases: the collector converts solar energy to thermal energy of the air, the chimney converts thermal energy to kinetic energy of airflow, and the turbine generators convert the kinetic energy of airflow to electric power.

Pretorius and Kröger [26] developed a detailed model to simulate the airflow and heat transfer in solar chimney power plants. In his model, the thermal storage is taken into consideration. Zhou et al. [27] proposed a compressible flow model to accurately simulate the velocity of flow.

In this work, thermal storage and air compressibility are not considered because the total potential power in a year is simply estimated in the analysis based on the annual and monthly global solar radiation. A simple mathematical model is presented, which is used to evaluate the performance of the SCPP. In the model, the air follows the ideal gas law, and the chimney wall is considered to be adiabatic and slippery. The heat gain of air in the collector is given by

$$c_p \dot{m} \Delta T = \eta_{coll} A_{coll} G \tag{1}$$

where c_p is specific heat capacity of air, ΔT is temperature difference between the collector outlet air and the ambient air, η_{coll} is collector efficiency, G is global solar radiation intensity, and the mass flow rate of operating air passing through the chimney, $\dot{m}_f$, can be calculated with the help of the following equation:

$$\dot{m} = \rho w_M A_c \tag{2}$$

where ρ is the density of air at the outlet of the solar collector, A_c is the chimney cross section, and w_M is the maximum vertical velocity of flow at the chimney inlet. The maximum vertical velocity is assumed to be obtained when the turbine is removed off and friction losses are neglected. w_M can be given by

$$w_M = \sqrt{2gH\frac{\Delta T}{T_0}} \tag{3}$$

According to Eqs. (1)–(3), w_M can further be written as,

$$w_M = \left(\frac{2gH\eta_{coll}A_{coll}G}{c_p \rho T_0 A_c}\right)^{1/3} \tag{4}$$

The dynamic pressure in the chimney under no load conditions is found to be equal to the pressure potential (available system pressure difference) [6]. The pressure potential is calculated by

$$\Delta p = \frac{1}{2}\rho w_M^2 \tag{5}$$

According to Bernardes et al. [28], the theoretical utilizable power taken up by the turbine is expressed as

$$P = \eta_{tg} \Delta p A_c w_M \alpha \sqrt{1-\alpha} = \frac{1}{2}\rho w_M^3 A_c \eta_{tg} \alpha \sqrt{1-\alpha} \tag{6}$$

Substituting Eq. (4) into Eq. (6), it can be written as

$$P = \frac{HA_{coll}G}{T_0} \cdot \frac{g\eta_{coll}\eta_{tg}\alpha\sqrt{1-\alpha}}{c_p} \tag{7}$$

where η_{tg} is mechanical efficiency of the turbine generators, and α is the ratio of pressure drop in the turbine to pressure potential. Von Backström and Fluri [29] reported that the optimum value of α is $(n-m)/(n+1)$, where m is pressure potential exponent, and n is pressure loss exponent. The value of α is typically a number between 2/3 and 1, and is equal to 2/3 when pressure potential is assumed to be constant. In reality, to calculate the power taken up by the turbine conveniently, a constant value is used in the models. Schlaich et al. [9] recommended a value of α equal to 0.8 while Bernardes et al. [28] recommended a value as high as 0.9. From Eq. (6), when α is assumed to be a constant, power production is proportional to the cube of velocity magnitude at the chimney inlet where the turbine generators are installed. In this model, the value of α is set at 0.9.

The physical properties of air are assumed to vary linearly with air temperature because of the low temperature range encountered. The heating process of the airflow in the collector can be treated as constant pressure expansion process [30]. Airflow density ρ can also be taken to be related by empirical relation for air properties [31] and is given by

$$\rho = 1.1614 - 0.00353(T - 300) \tag{8}$$

Total energy conversion efficiency of SCPP, η, can be expressed as the ratio of P to solar radiation radiated on solar collector,

$$\eta = \frac{P}{A_{coll}G} \tag{9}$$

Based on the above model, computation has been carried out to predict and analyze the SCPP performance.

5. Results and discussion

5.1. Performance of SCPP

To carry out the analysis of SCPP performance, we consider a reference 100 MW SCPP for an example, whose baseline parameters are given in Table 4. The SCPP has a collector 5650 m in diameter, and a chimney 1000 m high with a diameter of 80 m. In this model, the collector efficiency is assumed to be 65% [6,32]. Solar radiation intensity and atmospheric temperature are

Table 4
Baseline parameters of reference SCPP with 100 MW power output.

Parameter	Value	Unit
Collector diameter	5650	m
Chimney height	1000	m
Chimney diameter	80	m
Solar radiation intensity	800	W/m^2
Atmospheric temperature	20	°C
Collector efficiency	65	%
Temperature rise	17	°C
Density of air at collector outlet	1.13	kg/m^3
Maximum updraft velocity under no load condition	33.7	m/s
Updraft velocity under on load condition	10.7	m/s
Power output	100	MW
Total efficiency	0.5	%

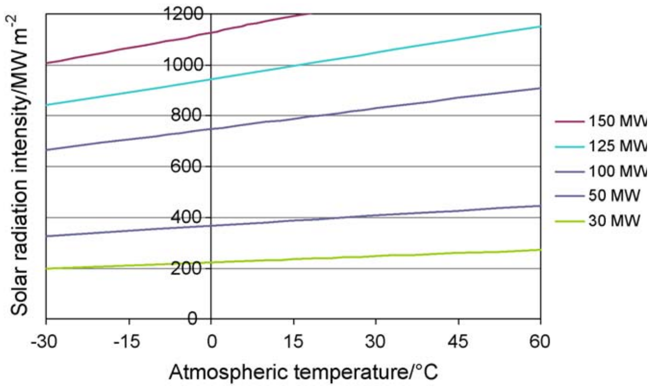

Fig. 4. Solar radiation intensity and atmospheric temperature versus power output.

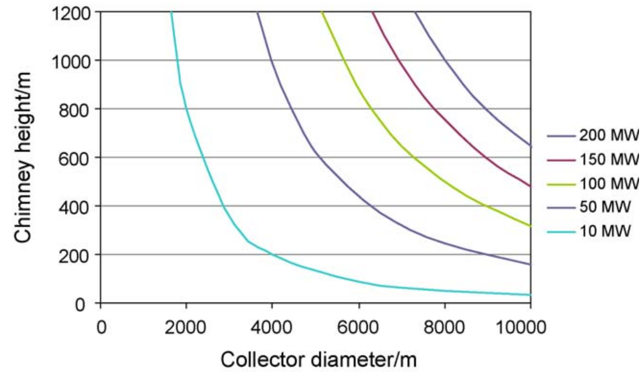

Fig. 5. Solar chimney height and collector diameter versus power output.

assumed to be 800 W/m^2 and 20 °C. The results show that the temperature rise in the air in the collector at 17 °C, gives a maximum updraft velocity 33.7 m/s under no load condition, while the updraft velocity under on load condition lies at 10.7 m/s. The total efficiency under these conditions is about 0.5%.

Figs. 4 and 5 show the variation of power output with collector diameter ranging from 2000 to 10000 m and chimney height from 35 to 1200 m, and with solar radiation intensity ranging from 200 W/m^2 to 1200 W/m^2 and ambient temperature from −30 °C to 60 °C. A height of 1200 m or higher can be reached for solar chimney by going along the surrounding mountain-topography [33] or using novel floating solar chimney technology [8]. The floating solar chimney will also not be damaged by possible natural disasters such as earthquakes [8]. These results show that the power output sharply increases with an increase in chimney height, collector area, and solar radiation intensity, but slowly reduces with an increase in atmospheric temperature based on Eq. (7). Substituting Eq. (3) into Eq. (6), it can also be rewritten as.

$$P = 2^{1/2}\left(gH\frac{\Delta T}{T_0}\right)^{3/2}\rho A_c \eta_{tg}\alpha\sqrt{1-\alpha} \quad (10)$$

From Eq. (10), the influence of atmospheric temperature on the power output will be much larger during night time without solar radiation input. This also shows that large diurnal temperature range is definitely a valuable resource for solar chimney power generation after sunset.

5.2. Performance of SCPP in Qinghai-Tibet Plateau

Fig. 6 shows the yearly power output from the reference SCPP at various locations of Qinghai-Tibet Plateau in comparison to other regions, whose conditions are presented in Table 2. As expected, the power output profile is uniform with solar radiation profile. In comparison with other regions, the difference between the value of power output and that of solar radiation in the plateau is slightly higher where the effect of lower atmospheric temperature is taken into consideration. Without any doubt, when the heat storage function and large diurnal temperature range effect is taken into consideration, the difference in the power outputs from SCPP in and out of Qinghai-Tibet Plateau will definitely be larger.

To analyze performance of SCPP in Qinghai-Tibet Plateau, three locations were selected, including a high solar radiation region, Lhasa in Tibet, a low solar radiation region, Xining in Qinghai, and another region not in the plateau, Guiyang. Their latitudes lie between N25° and N40°. The investigation from 1960 to 2002 shows global solar radiation in the Qinghai-Tibet Plateau has small yearly fluctuations around a average value [34]. In this work we takes the global solar radiation data from 1979 to 1981 being close

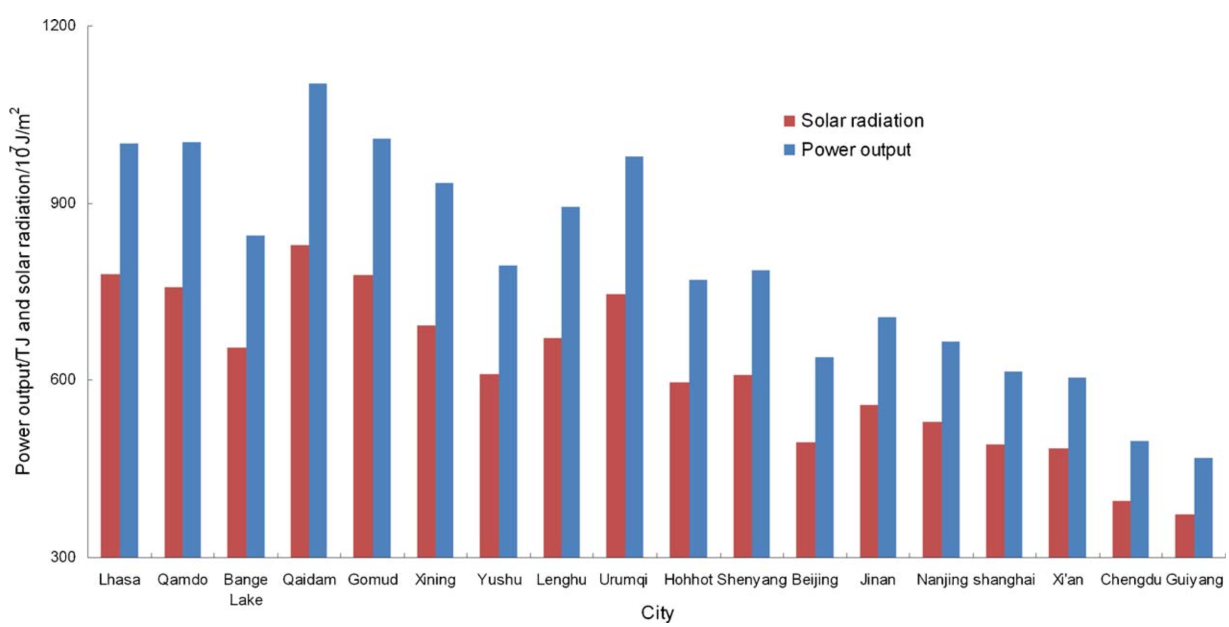

Fig. 6. Yearly power output from reference SCPP in various regions in and out of Qinghai-Tibet Plateau.

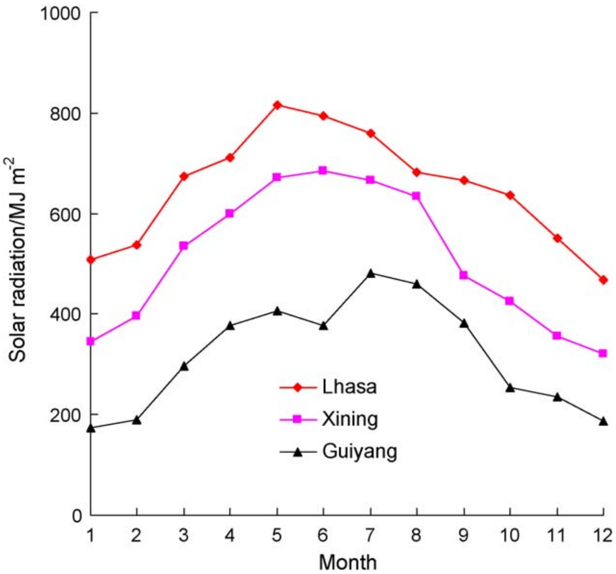

Fig. 7. Global solar radiations at three locations versus month.

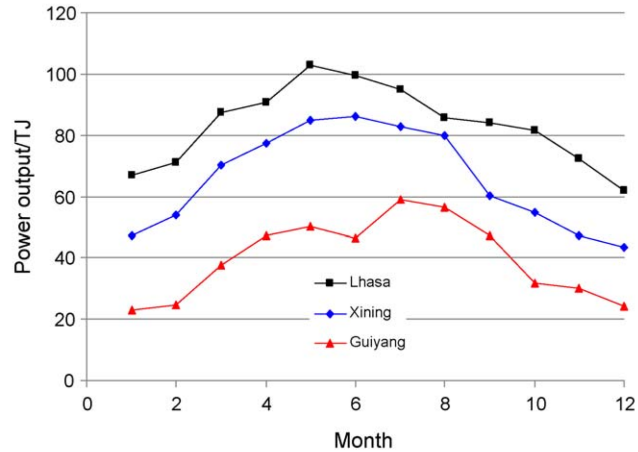

Fig. 9. Power outputs at three locations versus month of a year.

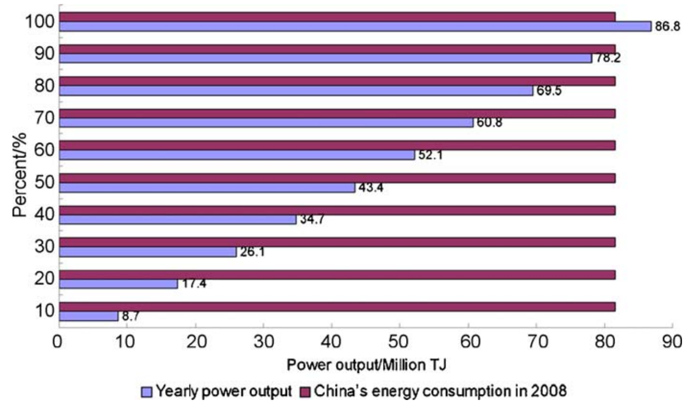

Fig. 10. Comparisons of yearly power output with various percent of SCPP construction region area to total plateau area and China's energy consumption in 2008.

to the average values as an example to perform analyses [3–4] (Figs. 7 and 8). The atmospheric temperatures refer to Ref. [35]. The results show that the three power output profiles show a uniform trend. The high power values are reached between April and September, while the profiles drop to the nadir in Jan and December (Fig. 9). The peak power reaches 103.4 TJ in May, 85.4 TJ in June, and 58.4 TJ in July respectively. The lowest value of 61.6 TJ in December of this year for Lhasa is even higher than the peak of 58.4 TJ for Guiyang. The annual global solar radiation for Lhasa and Xining is equal to 992.8 TJ, and 783.3 TJ, which is 2.1 times and 1.65 times more than that for Guiyang at 475.4 TJ respectively for the same year.

5.3. Power potential of SCPP in Qinghai-Tibet Plateau

According to the year 2001 statistical data, the population of Qinghai-Tibet Plateau was 12.05 million, with 64.32% of population distributed in the plateau and the rest on the plateau edge. This population in the plateau covering 26.8% of the total land of China only accounts for 0.94% of the total population of China which stood at 1276.3 million in 2001 [36]. In the plateau, the population density is very low, and majority of plateau land is unused. This is one reason and the advantage that can be taken to use the plateau lands for SCPP construction and installation.

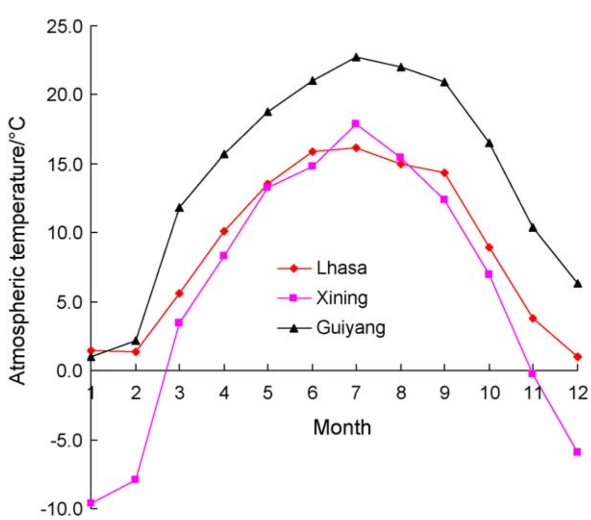

Fig. 8. Atmospheric temperatures at three locations versus month.

The potential energy production is estimated based on annual global solar radiation of 6500 MJ/m^2, and mean atmospheric temperature of 5 °C. Fig. 10 presents variation in yearly total potential power output with percent of SCPP construction region area to the total plateau area from 10% to 100% and compares these data with China's energy consumption in 2008 at 81.6 million TJ [35]. This figure shows that when all the regions of Qinghai-Tibet Plateau are used as construction sites of SCPP, the yearly total power from SCPP which could reach 86.8 million TJ is enough to satisfy the energy need of the whole country in 2008, however it is unrealistic to cover solar collector in the whole plateau. When 10% to 20% of land in the plateau could have been used for SCPP locations, the yearly power could have been between 8.7 million TJ and 17.4 million TJ, accounting for 10.7–21.3% of China's energy consumption in 2008. This shows that SCPP in the plateau can support the development of China together with other renewable energy resources such as hydroelectric power, wind power, biofuel, and, geothermal energy.

6. Conclusion

A mathematical model has been developed for air flow in SCPP in this work. SCPP performances were investigated with the model, and the results were then compared for different regions with the

almost same latitude. The following conclusions can be drawn from the analyses:

(1) There is vast land, abundant solar radiation, high direct solar radiation, low ambient temperatures, large diurnal temperature ranges, lots of salt lakes in Qinghai-Tibet Plateau. The Plateau is therefore suitable for construction sites of SCPP for utilizing local solar radiation. Additionally, salt lakes in the plateau can also be used as heat storage system for SCPP to control daily power output profile and increase the total power output by enlarging receiving surface of solar radiation.
(2) Power output increases with an increase in chimney height and collector area. It also increases with an increase in solar radiation, but slowly decreases with an increase in atmospheric temperature during day time. While, atmospheric temperature has a larger influence on the power output during night time.
(3) The power output of SCPP in Qinghai-Tibet Plateau is far more than that of the same latitude regions not in the plateau. The result may be attributed to the high solar radiation.
(4) The yearly total power potential for SCPP in Qinghai-Tibet Plateau is estimated to be 86.8 million TJ. When 10–20% of the plateau land is used for SCPP locations, the yearly power production can reach between 8.7 million TJ and 17.4 million TJ. This figure can account for 10.7–21.3% of China's energy consumption. This shows that SCPP in the plateau can support the local and national development together with other renewable energy resources.

Acknowledgement

This research has been supported by the National Natural Science Foundation of China under Grant No. 50908094, and the Youth Chenguang Project of Science and Technology of Wuhan City of China under Grant No. 201050231076.

References

[1] Qinghai-Tibet Railway. http://baike.baidu.com/view/2580.htm?fr=ala0.
[2] Zhou XP, Xiao B, Ochieng RM, Yang JK. Utilization of carbon-negative biofuels from low-input high-diversitygrassland biomass for energy in China. Renewable and Sustainable Energy Reviews 2009;13:479–85.
[3] Zhang SY. Sunlight utilization and its efficiency improvement measure of plants in Qinghai-Tibet Plateau. Journal of Qinghai Environment 1993;3:81–6 [in Chinese].
[4] Dai JX. Climate of Qinghai-Tibet Plateau. China, Beijing: Meteorology Publishing House; 1990 [in Chinese].
[5] Zuo DK, Wang YX, Chen JS. Characteristics of the distribution of total radiation in China. Acta Meteorologica Sinica 1963;33:78–96 [in Chinese].
[6] Schlaich J. The solar chimney: electricity from the sun. Stuttgart, Germany: Edition Axel Menges; 1995.
[7] Günther H. In hundert Jahren–Die künftige Energieversorgung der Welt (In hundred years–Future energy supply of the world). Stuttgart: Kosmos, Franckh'sche Verlagshandlung; 1931.
[8] Zhou XP, Yang JK, Wang F, Xiao B. Economic analysis of floating solar chimney power plant. Renewable and Sustainable Energy Reviews 2009;13:736–49.
[9] Schlaich J, Bergermann R, Schiel W, Weinrebe G. Design of commercial solar updraft tower systems-utilization of solar induced convective flows for power generation. Journal of Solar Energy Engineering 2005;127:117–24.
[10] Haaf W, Friedrich K, Mayr G, Schlaich J. Solar chimneys, part I: principle and construction of the pilot plant in Manzanares. International Journal of Solar Energy 1983;2:3–20.
[11] Haaf W. Solar chimneys, part II: preliminary test results from the Manzanares pilot plant. International Journal of Solar Energy 1984;2:141–61.
[12] Krisst RJK. Energy transfer system. Alternative Sources of Energy 1983;63:8–11.
[13] Kulunk H. A prototype solar convection chimney operated under Izmit conditions. In: Veiroglu TN, editor. Proceedings of the 7th Miami International Conference on Alternative Energy Sources. 1985. p. 162.
[14] Pasumarthi N, Sherif SA. Experimental and theoretical performance of a demonstration solar chimney model—Part II: experimental and theoretical results and economic analysis. International Journal of Energy Research 1998;22:443–61.
[15] Zhou XP, Yang JK, Xiao B, Hou GX. Experimental study of the temperature field in a solar chimney power setup. Applied Thermal Engineering 2007;27:2044–50.
[16] Ketlogetswe C, Fiszdon JK, Seabe OO. Solar chimney power generation project—the case for Botswana. Renewable and Sustainable Energy Reviews 2008;12:2005–12.
[17] Ferreira AG, Maia CB, Cortez MFB, Valle RM. Technical feasibility assessment of a solar chimney for food drying. Solar Energy 2008;82:198–205.
[18] Koyun A, Üçgül I, Acar M, Şenol R. Güneş Bacası Sisteminin Termal Özet Dizaynı. Tesisat Mühendisliği Dergisi 2007;98:45–50. available at: http://www.mmoistanbul.org/yayin/tesisat/98/6.
[19] Dennis C. Solar energy: radiation nation. Nature 2006;443:23–4.
[20] Davey RC. Device for generating electricity from solar power. WO 2008/022372 A1; 28 February 2008.
[21] Zhou XP, Yang JK, Xiao B, Li J. Night operation of solar chimney power system using solar ponds for heat storage. International Journal of Global Energy Issues 2009;31:193–207.
[22] Zhang YL, Li BY, Zheng D. A distribution on the boundary and area of the Tibetan Plateau in China. Geographical Research 2002;21:1–10 [in Chinese].
[23] Zheng XY, Zhang MG, Xu C, Li BX. China salt lake log. China, Beijing: Science Publishing Company; 2002 [in Chinese].
[24] Zhou XP, Yang JK, Ochieng RM, Xiao B. Numerical investigation of a plume from a power generating solar chimney in an atmospheric cross flow. Atmospheric Research 2009;91:26–35.
[25] Zhou XP, Yang JK, Xiao B. Solar power generation and use of grassland in ecology management. In: Schröder HG, editor. Grasslands: ecology, management and restoration. Hauppauge, NY, USA: Nova Science Publishers Inc.; November 2008, ISBN: 9781606920244.
[26] Pretorius JP, Kröger DG. Solar chimney power plant performance. Journal of Solar Energy Engineering 2006;128:302–11.
[27] Zhou XP, Yang JK, Wang JB, Xiao B, Hou GX, Wu YY. Numerical investigation of a compressible flow through solar chimney. Heat Transfer Engineering 2009;30:670–6.
[28] Bernardes MA, dos S, Voss A, Weinrebe G. Thermal and technical analyzes of solar chimneys. Solar Energy 2003;75:511–24.
[29] Von Backström TW, Fluri TP. Maximum fluid power condition in solar chimney power plants—an analytical approach. Solar Energy 2006;80:1417–23.
[30] Gannon AJ, Von Backström TW. Solar chimney cycle analysis with system loss and solar collector performance. Journal of Solar Energy Engineering 2000;122:133–7.
[31] Zhou XP, Yang JK, Xiao B, Hou GX, Xing F. Analysis of chimney height for solar chimney power plant. Applied Thermal Engineering 2009;29:178–85.
[32] Larbi S, Bouhdjar A, Chergui T. Performance analysis of a solar chimney power plant in the southwestern region of Algeria. Renewable and Sustainable Energy Reviews 2010;14:470–7.
[33] Bonnelle D. Solar chimney, water spraying energy tower, and linked renewable energy conversion devices: presentation, criticism and proposals. Doctoral thesis. Lyon 1, France: University Claude Bernard; July 2004. Registration Number: 129-2004.
[34] Chen F, Ma YF, Li WQ. Distribution characteristics of solar radiation over Qinghai Plateau. Meteorological Science and Technology 2005;33:231–4 [in Chinese].
[35] National Bureau of Statistics of China. China Energy Statistical Yearbook 2009. Beijing: China Statistical Press; 2009.
[36] Zhang YL, Zhang W, Bai WQ, Li SC, Zheng D. An analysis of statistical data about Tibetan Plateau in China—a case study on population. Progress in Geography 2005;24:11–21 [in Chinese].